Oleic acid enhances proliferation and calcium mobilization of CD3/CD28 activated CD4+ T cells through incorporation into membrane lipids

Hegedus, J.H. von; Jong, A.J. de; Hoekstra, A.T.; Spronsen, E.; Zhu, W.H.; Cabukusta, B.; ... ; Ioan-Facsinay, A.

Basic

European Journal of **Immunology**
Clinical·Basic·Translational

Molecular immunology and signaling

Research Article

Oleic acid enhances proliferation and calcium mobilization of CD3/CD28 activated CD4+ T cells through incorporation into membrane lipids

Johannes Hendrick von Hegedus[1,2], Anja J. de Jong[1], Anna T. Hoekstra[3,4], Eric Spronsen[1], Wahwah Zhu[1], Birol Cabukusta[5], Joanneke C. Kwekkeboom[1], Marieke Heijink[6], Erik Bos[7], Celia R. Berkers[3], Martin A. Giera[6], Rene E. M. Toes[1] ⓘ *and Andreea Ioan-Facsinay[1]*

[1] Department of Rheumatology, Leiden University Medical Center, Leiden, The Netherlands

[2] Department of Clinical Sciences, Faculty of Veterinary Medicine, Utrecht University, Utrecht, The Netherlands

[3] Biomolecular Mass Spectrometry and Proteomics, Bijvoet Center for Biomolecular Research, Utrecht University, Utrecht, The Netherlands

[4] Division of Endocrinology, Department of Medicine, Leiden University Medical Center, Leiden, The Netherlands

[5] Department of Cell and Chemical Biology, Oncode Institute, Leiden University Medical Center, Leiden, The Netherlands

[6] Center for Proteomics and Metabolomics, Leiden University Medical Center, Leiden, The Netherlands

[7] Department of Cell and Chemical Biology, Leiden University Medical Center, Leiden, The Netherlands

Unsaturated fatty acids (UFA) are crucial for T-cell effector functions, as they can affect the growth, differentiation, survival, and function of T cells. Nonetheless, the mechanisms by which UFA affects T-cell behavior are ill-defined. Therefore, we analyzed the processing of oleic acid, a prominent UFA abundantly present in blood, adipocytes, and the fat pads surrounding lymph nodes, in CD4+ T cells. We found that exogenous oleic acid increases proliferation and enhances the calcium flux response upon CD3/CD28 activation. By using a variety of techniques, we found that the incorporation of oleic acid into membrane lipids, rather than regulation of cellular metabolism or TCR expression, is essential for its effects on CD4+ T cells. These results provide novel insights into the mechanism through which exogenous oleic acid enhances CD4+ T-cell function.

🖥 Additional supporting information may be found online in the Supporting Information section at the end of the article.

Introduction

CD4+ T cells play a central role in many immune reactions either directly through soluble mediators or indirectly by providing help to other immune cells [1]. The activation and proliferation of CD4+ T cells are, therefore, essential for proper immune regulation. Upon activation, CD4+ T cells undergo a plethora of functional and metabolic changes that affect cell size, signaling pathways, and nutrient uptake. Fatty acids (FA) are crucially involved in these processes, and therefore their uptake and processing should be tightly regulated [2–4].

Dietary FA have been shown to play a role in a variety of inflammatory diseases including diabetes [5], Crohn's disease [6], and arthritis [7]. Although their impact reaches beyond the regulation of immune responses, dietary FA have been directly implicated in the modulation of human T-cell function and activation [8]. Several studies report that cellular FA can disrupt the integrity of the T-cell receptor (TCR) complex [9, 10] and can affect

Correspondence: Johannes Hendrick von Hegedus
e-mail: j.h.vonhegedus@uu.nl

signaling proteins downstream of the TCR [10, 11] thereby modifying T-cell function. A link between FA and CD4$^+$ T-cell function is also suggested by the interplay between TCR activation and the upregulation of genes involved in FA biosynthesis. In addition, genetic inactivation of FA biosynthesis has been shown to hinder a proper T-cell response [12].

T cells are often reliant on FA for their energy requirements [13–16] and lipid biosynthesis [13–17]. Although FA required for T-cell function can be synthesized de novo [18], they can also be derived from exogenous sources [19]. CD4$^+$ T cells possess fatty-acid-binding proteins required for FA uptake [19] and their expression is, for example, crucial for the formation of long-term tissue-resident memory responses [20]. Likewise, flow cytometric analysis using fluorescent lipid probes showed that the T-cell activation status directly correlated with the amount of FA they have taken up [21].

Oleic acid represents approximately 30% of the total nonesterified plasma FA in healthy individuals making it the most abundant free FA, [22]. Relatively high amounts of oleic acid have also been found in the infrapatellar fat pad [23], synovial fluid (SF) [23], and adipocytes [24, 25], suggesting that oleic acid is readily available within the T-cell microenvironment. Studies conducted on oleic acid have revealed multiple effects on various immune cells [26] including CD4$^+$ T cells [27]. Furthermore, increased concentrations of oleic acid have been associated with different inflammatory diseases [6, 23].

Studies on the effect of exogenous FA on T-cell function mostly focused on dietary unsaturated fatty acids (UFA) because of their association with inflammatory diseases [28]. In general, these studies concluded that low concentrations of FA can increase the proliferation of T cells [25, 29, 30]. However, changes in metabolism or cellular signaling were not evaluated and the mechanism used by exogenous FA to modulate CD4$^+$ T-cell function is not well known. Therefore, we evaluated the fate of exogenous FAs in human CD4$^+$ T cells and their effect on TCR signaling and proliferation by focusing on oleic acid, a model lipid for exogenous UFA.

Results

Oleic acid enhances proliferation of CD4$^+$ T cells

The effect of oleic acid on CD4$^+$ T-cell proliferation was examined first using a 3H-thymidine assay. A clear dose-dependent increase in proliferation of αCD3 /αCD28 stimulated CD4$^+$ T cells upon oleic acid incubation was observed (Fig. 1A). Interestingly, the effect on the proliferation was still present 3 days after removal of the oleic acid at concentrations of 1 μg/mL or higher (Fig. 1B). Moreover, the increased proliferation in response to oleic acid was already detectable after 24 h (Fig. 1C). To assess the effect of oleic acid on cell division, a cell trace violet (CTV) staining was performed and enhanced cell division was detected both on day 1 (Fig. 1D) and day 4 (Fig. 1E). To further define the functional properties of these αCD3/αCD28-stimulated CD4$^+$ T cells

in the presence of oleic acid, IL-2, IFN-γ, IL-10, IL-4, IL-5, IL-6, and TNF-α concentrations were measured in the culture medium. On day one IFN-γ, IL-10, IL-4, and TNF-α were higher in the oleic acid (1 μg/mL) treated cells compared with vehicle control (Fig. S3A and B). In contrast, oleic acid treatment did not increase IL-2 release on day 1. On day 4, low concentrations of oleic acid (1ug/mL) increased the IL-2 levels in the medium but high concentrations (10 μg/mL) reduced it. Collectively, our data indicate that oleic acid dose-dependently enhances the proliferation of CD4$^+$ T cells and this is an early event.

Oleic acid is incorporated into membrane lipids

To get a better insight into how oleic acid is processed by CD4$^+$ T cells, oleic acid-treated CD4$^+$ T cells were analyzed using DMS-ESI(±)MS/MS (Lipidyzer platform). The most abundant lipid species in the membrane of the activated CD4$^+$ T cells were 42.62% sphingomyelin (SM), 16.72% phosphatidylethanolamine (PE), 12.21% phosphatidylcholine (PC) (Fig. S1A). The total amount of membrane lipids was comparable before and after 24 h of preincubation with oleic acid (Fig. S1B); however, within the higher-order lipid species that contained at least one chain of oleic acid (18:1), an increase was observed upon treatment. More specifically membrane lipids, SM, PC, PE, diglyceride (DAG) and to a lesser extent ceramide (CER) increased when CD4$^+$ T cells were treated with oleic acid. An increase in non-membrane lipid species free fatty acids (FFA) and triglyceride (TG) was also observed (Fig. 2A). Because the highest increase of oleic acid was observed in the PC fraction we further dissected the individual PC that contained an oleic acid moiety and found that multiple PC increase approximately by 150–276%. Relatively PC(18:1_18:1) increased the most when cells were incubated with 10 μg/mL oleic acid this PC increased by 1134%. (Fig. 2A). To assess if the increase of membrane lipids containing oleic acid was due to the incorporation of the added oleic acid or rather endogenous oleic acid synthesis, ^{13}C-labeled oleic acid (^{13}C-OA) treated cells were analyzed by LC-FT/MS. Approximately 15–40% of the added ^{13}C-OA could be traced back in the cells after 24 h. In concordance with the previous experiment, the highest percentage of ^{13}C-OA was found in the PC in the form of PC(18:1_18:1). ^{13}C-OA could be also be traced back in PC(16:0_18:1), PC(20:4_18:1), PC(18:1_18:2) and PC(18:0_18:1) (Fig. 2B).

To validate and expand these findings, we employed alkyne-modified oleic acid (OA(17yne)), which allows visualization by attaching an azide-containing fluorophore through a copper-catalyzed click reaction [31]. OA(17yne) is biorthogonal allowing 24 h incubation of this compound without affecting the copper-reactive ethynyl group (ethynyl group is highlighted in green, Fig. 2D) [32]. After 24 h treatment with OA(17yne), lipids were extracted and a click reaction was performed with the fluorogenic coumarin-azide before thin-layer chromatoraphy separation (Fig. 2C). This analysis further confirmed that oleic acid is incorporated into four different lipid classes. The visualized bands were subsequently isolated and analyzed using LC/MS/MS (Sciex
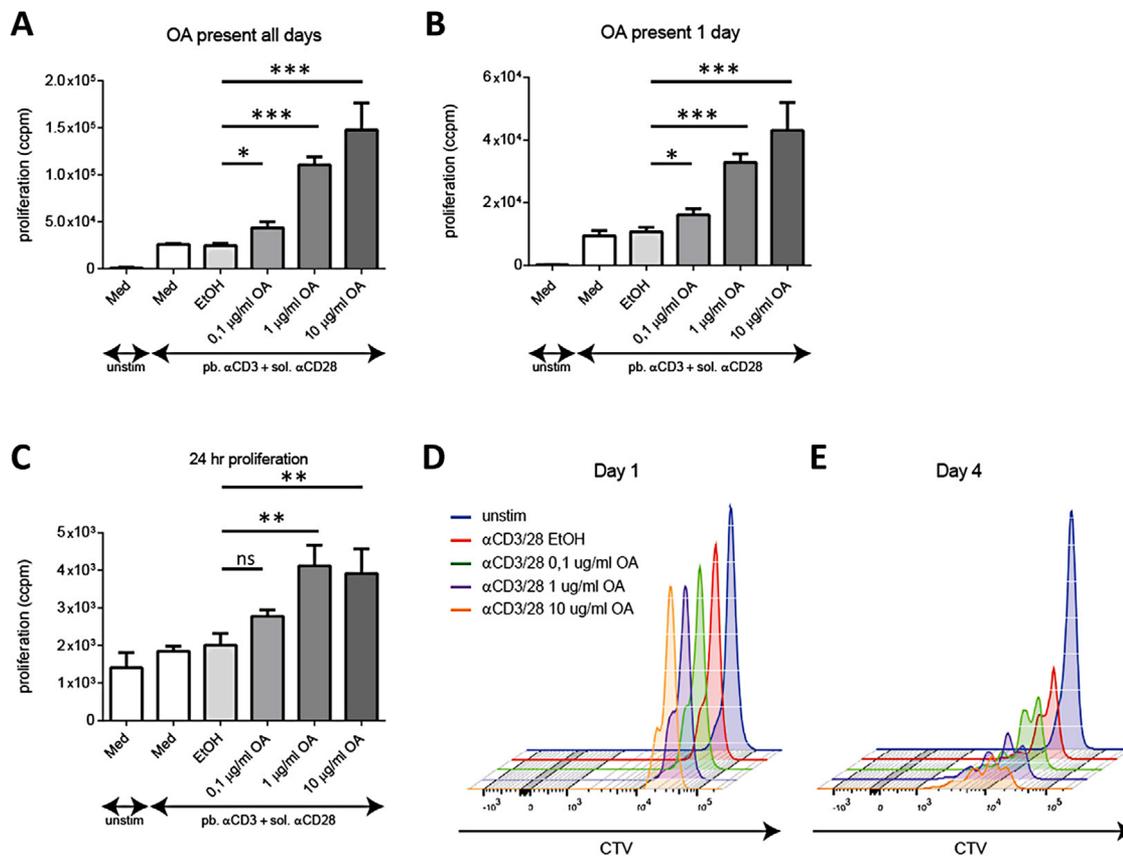
Figure 1. Proliferation of CD3/CD28 activated CD4+ T cells incubated with different concentrations of oleic acid. Isolated CD4+ T cells labeled with 0.5 µCi 3H-thymidine were incubated with 0.1, 1, or 10 µg/mL oleic acid (OA) or control, in the presence of plate-bound (pb) αCD3 and soluble (sol) αCD28. Lash and glow luminescence were measured using a 1450 LSC & luminescence counter. (A) Proliferation was measured after 4 days in the presence of oleic acid or (B) washed away after 24 h. (C) Proliferation directly after 24 h incubation of oleic acid. Data are shown as mean + SD of triplicates from one representative donor in total four donors were used in four independent experiments. (D) Isolated CD4+ T cells labeled with cell trace violet (CTV) were incubated with 0.1, 1, or 10 µg/mL oleic acid or control, in the presence of pb αCD3 and soluble sol αCD28. Representative plots of CTV dilutions after 1 day or (E) 4 days. Data are shown from one representative donor of in total four donors that were performed in four independent experiments. A paired students T-test was performed ns >0.05, *$p < 0.05$; **$p < 0.01$; ***$p < 0.001$. Ccpm = corrected counts per minute

TripleTOF 6600), where the same PC subspecies identified by ^{13}C-OA labeling as well as SM(18:1-16:0) and SM(18:1-24:0) were identified in bands 3 and 4. Bands 1 and 2 could not be identified due to technical difficulties (Fig. 2C). Taken together, these experiments show that exogenous oleic acid and OA(17yne) were incorporated by proliferating CD4+ T cells into membrane lipids.

The subcellular localization of oleic acid could shed light on the possible mechanism by which membrane lipids affect proliferation. Fluorescence labeling of OA(17yne) using click chemistry also allows its visualization by fluorescent microscopy as well as correlative light and electron microscopy. By performing correlative light and electron microscopy, we could correlate OA(17yne) localization to mitochondria (Fig. 2D). To validate if OA(17yne) is localized at mitochondria, a co-staining with Mitotracker was performed and multiple Z-stack images were taken by confocal microscopy. These images confirm the co-localization of the OA(17yne) with the Mitotracker. In addition, nuclear envelope staining was also visible around the DAPI-stained nucleus

(Fig. 2E). The subcellular localization of oleic acid seems to be most prominent in the membrane-dense organelles such as mitochondria and nuclear membrane.

We could, however, not exclude the possibility that the lack of fluorescent signal in other membranes was due to either dilution or the duration of oleic acid incubation. Since oleic acid tends to diffuse into lipid membranes we expect it to also incorporate into the cell-surface membranes, which could affect the surface TCR and downstream signaling. To address this possibility, we treated CD4+ T-cell with oleic acid and determined the surface expression of different TCR signaling molecules. The main components of the TCR signaling complex, TCRα/β, and CD3, together with CD69 and CD25, which are upregulated upon T-cell activation, were evaluated. Activation of CD4+ T cells decreased TCR and CD3 expression (Fig. S2A), while oleic acid had no significant effect on these molecules (Fig. S2B). Activation makers CD69 and CD25 increased upon activation (Fig. S2A) while oleic acid had no significant effect on these molecules (Fig. S2B).
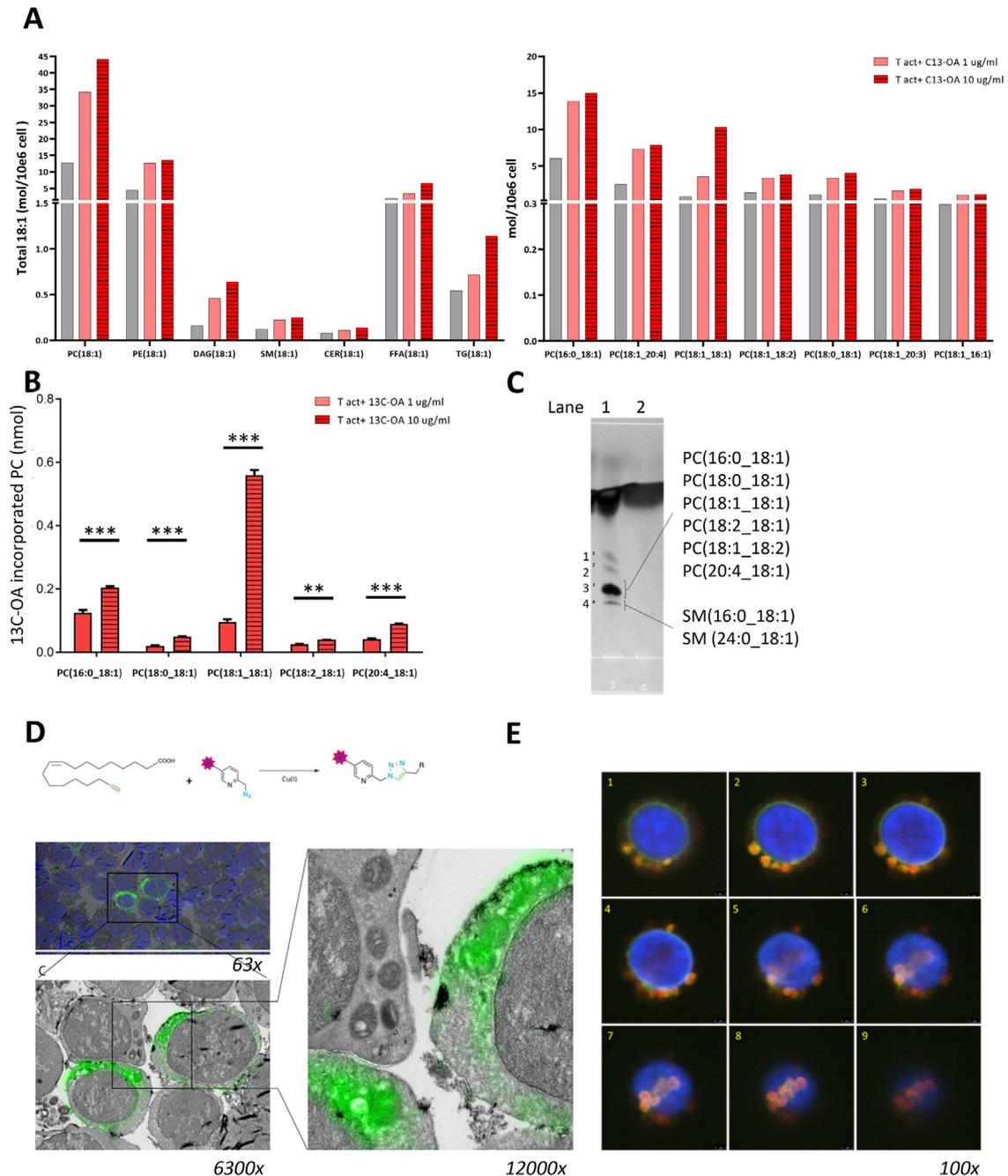
Figure 2. Oleic acid incorporation into membrane lipids of CD3/CD28 activated CD4+ T cells incubated with different concentrations of oleic acid. (A) The lipid fraction of plate-bound (pb) αCD3 and soluble (sol) αCD28 activated CD4+ cells pretreated for 24 h with oleic acid (1–10 μg/mL). Total concentration of all 18:1 (oleic acid moiety) containing membrane lipids. CER, ceramides; DAG, diacylglycerides; FFA, free fatty acids; PC, phosphatidylcholine; PE, phosphatidylethanolamine; SM, sphingomyelin; and TG, triacyltriglycerides. Second graph shows individual oleic acid (18:1) containing PC quantified by DMS- ESI(±)MS/MS (Lipidyzer) in one donor. (B) ^{13}C-OA incorporation in PC measured by LC-FT/MS mean + SD from triplicate of one donor. A paired students T-test was performed (C) Visualization by UV of TLC separated lipid fraction of (Z)-octadec-9-en-17-ynoic acid ((OA)17-yne) treated CD4+ T cells of one donor. Lane 1 contains lipid fraction of OA(17-yne) treated cells, second lane contains lipid fraction from oleic acid-treated cells. Isolated bands were further analyzed using LC/MS/MS resulting in the identification of specific species within the bands. (D) Reaction formula showing the formation of covalent bonds between OA(17yne) and conjugate-azide through a copper-catalyzed click-reaction. Confocal and EM images of stimulated CD4+ T cells treated for 24 h with OA(17-yne) followed by 30 min with AF488-azide and DAPI. Image overlay of the confocal image with an EM image (6300×), overlay of confocal image and an EM image (12,000×), DAPI not shown (E). Z-stack confocal images 63×. DAPI (blue), Mitotracker (red), and OA-AF488 (green). All data depicted was acquired in independent experiments using different donors. ns >0.05, *$p < 0.05$; **$p < 0.01$; ***$p < 0.001$

Oleic acid is incorporated in oleoyl-L-carnitine and not used as an energy substrate

High concentrations of oleic acid within the mitochondrial membrane could potentially indicate that oleic acid is used as an energy substrate. To study if the effect of oleic acid on CD4$^+$ T cells is mainly due to its use as an energy source, LC-MS-based metabolomics was performed. A selection of carbohydrates, nucleotides, lipids, amino acids, vitamins, and energy metabolites were measured to map the metabolic state of the CD4$^+$ T cells. Preincubation with oleic acid did not increase these metabolites in a substantial way except for oleoyl-L-carnitine (Fig. 3A). To further confirm these findings ^{13}C-OA was used to track the fate of oleic acid in proliferating CD4$^+$ T cells. LC-MS analysis was performed on ^{13}C-OA treated cells. In agreement with the previous results, ^{13}C-OA was incorporated into oleoyl-L-carnitine but not in the other analyzed metabolites of the TCA cycle (Fig. 3B). Finally, to exclude that oleic acid was used as an energy substrate, glycolysis, and mitochondrial respiration were measured using Seahorse technology. Glycolysis by analyzing the extracellular acidification rate (ECAR) and measures mitochondrial oxidative phosphorylation based on the oxygen consumption rate (OCR). Activation of CD4$^+$ T cells enhanced glycolysis without affecting mitochondrial respiration. Both metabolic pathways were unaffected by oleic acid treatment (Fig. 3C).

Oleic acid does not affect PLCγ1 or ZAP70 phosphorylation

Because the data described above indicate that TCR expression is not affected by oleic acid (Fig. S2), we further investigated whether TCR-mediated signaling directly downstream of the TCR was affected by oleic acid incubation. To this end, phosphorylation of ZAP70 and PLCγ1, two central steps in the TCR-signaling cascade, were evaluated in CD4$^+$ T cells. The expression of p-ZAP70 increased upon αCD3 /αCD28 stimulation. However, there was no significant change in the expression of p-ZAP70 following 24 h preincubation with 1 μg/mL oleic acid (Fig. 4A and B). Similarly, no significant effect on p-PLCγ1 was observed after preincubation with oleic acid after 30 s. A slight but significant reducing trend was observed on PLCγ1 phosphorylation after 5 min of activation. Together, these data indicate no significant changes in early TCR signaling events upon oleic acid treatment (Fig. 4B).

Oleic acid enhances calcium mobilization in CD4$^+$ T cells

As oleic acid treatment does not affect PLCγ1 and ZAP70 phosphorylation, we hypothesized that it influences CD4$^+$ T-cell proliferation by influencing downstream events of PLCγ1 and ZAP70 phosphorylation, such as calcium flux. In experiments performed with 11 different donors, we found that pre-incubation with oleic acid enhances calcium flux response as observed in the height

and the slope of the peaks (Fig. 5A and B), indicating that oleic acid could potentially influence proliferation through enhanced calcium release. To address the question of whether the observed calcium mobilization to the cytosol depended on extracellular sources or intracellular stores, chelator ethylene glycol tetra acetic acid (EGTA) was used to remove free Ca^{2+} from the medium. We found that removing Ca^{2+} in the medium by EGTA inhibited the calcium flux responses of CD4$^+$ T cells during the first 24 h and that the presence of oleic acid slightly increased the calcium mobilization (Fig. S4A and B). This suggests that the effect of oleic acid on Ca^{2+} mobilization depends at least partially on intracellular Ca^{2+} stores.

Inhibition of sphingomyelin synthase by D609 decreased the effect of oleic acid on proliferation and calcium mobilization

The calcium channels that facilitate the increase of intracellular calcium concentration are located within the membrane. These membranes consist of lipids such as PC, PE, and SM. Our data indicate that exogenous oleic acid is first converted into membrane lipids before incorporation into the different membrane fractions of CD4$^+$ T cells (Fig. 2). The incorporation of oleic acid into membrane lipids is a result of a series of enzymatic conversions that can be partially inhibited by an inhibitor of sphingomyelin synthase (D609) (summarized in Fig. 6A). To determine if the incorporation of oleic acid into membrane lipids is essential for the effects observed on proliferation and calcium fluxes, D609 was used to inhibit this process. In our hands, incubation with D609 (75 μM) reduced the amount of oleic acid-containing membrane lipid species, except for CER which slightly increased. Furthermore D609 (75μM) reduced the amount of all oleic acid containing PC (Fig. S2C). Calcium flux peak height and slope of activated CD4$^+$ T cells were also reduced in D609-treated cells (Fig. 6D and E). Taken together we conclude that incorporation of oleic acid into membrane lipids is essential for the effect of oleic acid on CD4$^+$ T-cell proliferation and calcium release.

Discussion

In this study, we investigated the mechanism underlying the enhancing effect of exogenous oleic acid on CD4$^+$ T-cell proliferation. Our data shows that exogenous oleic acid can affect T-cell proliferation. Additionally, our data also indicates that the effect of oleic acid is mediated through its incorporation into membrane lipids, thereby allowing enhanced intracellular calcium signaling responses, rather than through enhanced TCR-signaling or modulation of metabolic pathways.

Several studies on oleic acid have demonstrated its diverse effects on various immune cells [26], including CD4$^+$ T cells [27]. In these studies, it has been reported that oleic acid can boost the proliferation of human lymphocytes via increased intracellular calcium mobilization thereby increasing the IL-2 expression
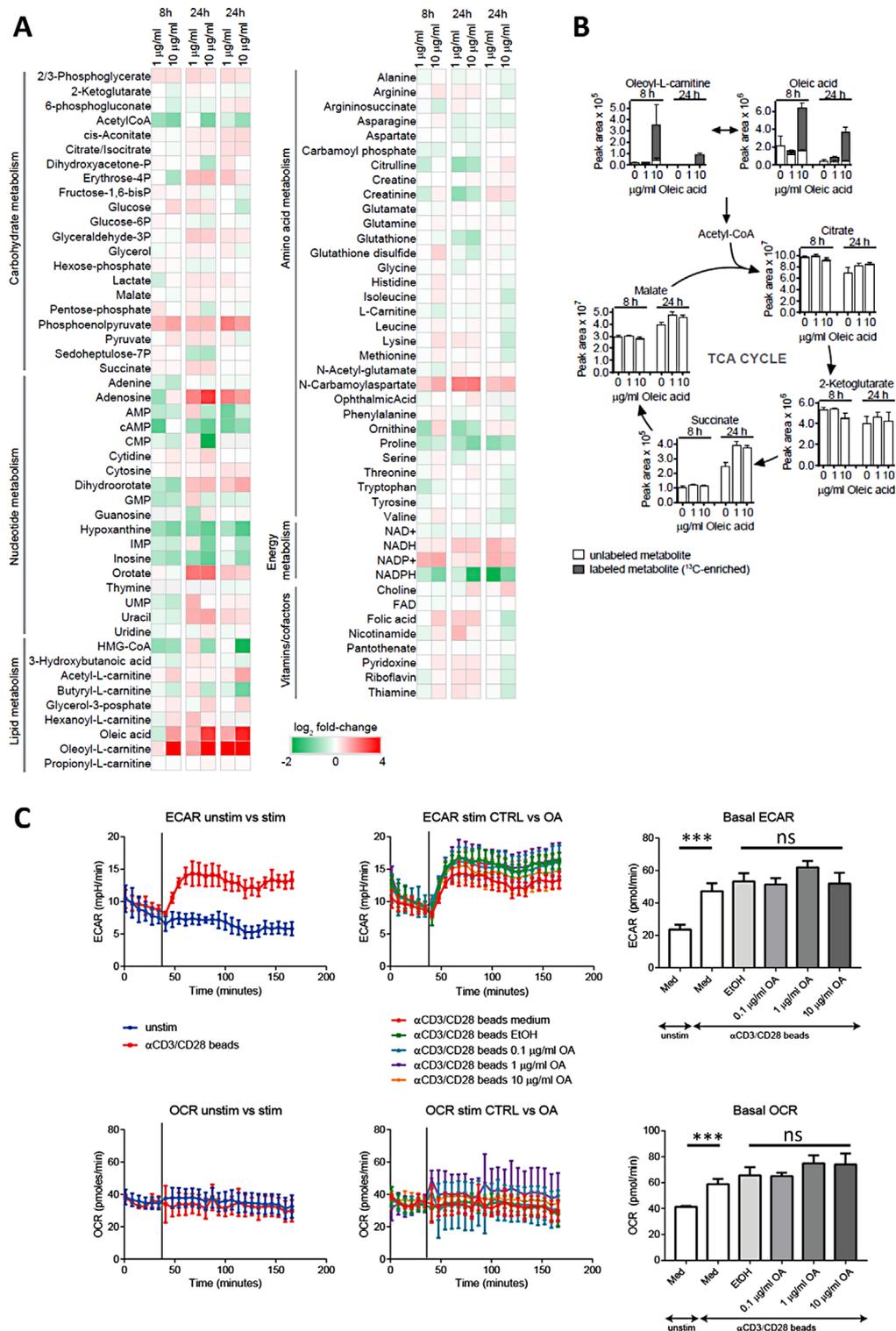
Figure 3. LC-MS-based metabolomics, extracellular acidification rate (ECAR), and mitochondrial oxidative phosphorylation (OCR) of CD3/CD28 activated CD4$^+$ T cells incubated with different concentrations of oleic acid. CD4$^+$ T cells were incubated with 100 ng/mL, 1 µg/mL, and 10 µg/mL oleic acid or vehicle control in the presence of plate-bound (pb) αCD3 and soluble (sol) αCD28. (A) LC-MS-based metabolomics was performed, in green the metabolites decreased, and in red the ones that increased compared with vehicle control. (B) LC-MS analysis was performed on ^{13}C-OA treated cells and the presence of unlabeled and labeled metabolites was determined. White bars represent unlabeled metabolites and grey bars labeled metabolites. TCA, tricarboxylic acid cycle. (C) ECAR and mitochondrial OCR were measured 200 min after activation with pb αCD3 and sol αCD28 (indicated by line). Data are shown as mean + SD of quintuplets of one representative donor of in total four donors in four independent experiments, LC-MS analysis of all samples was performed in one batch. A paired students *T*-test was performed ns >0.05, *P < 0.05; **p < 0.01; ***p < 0.001
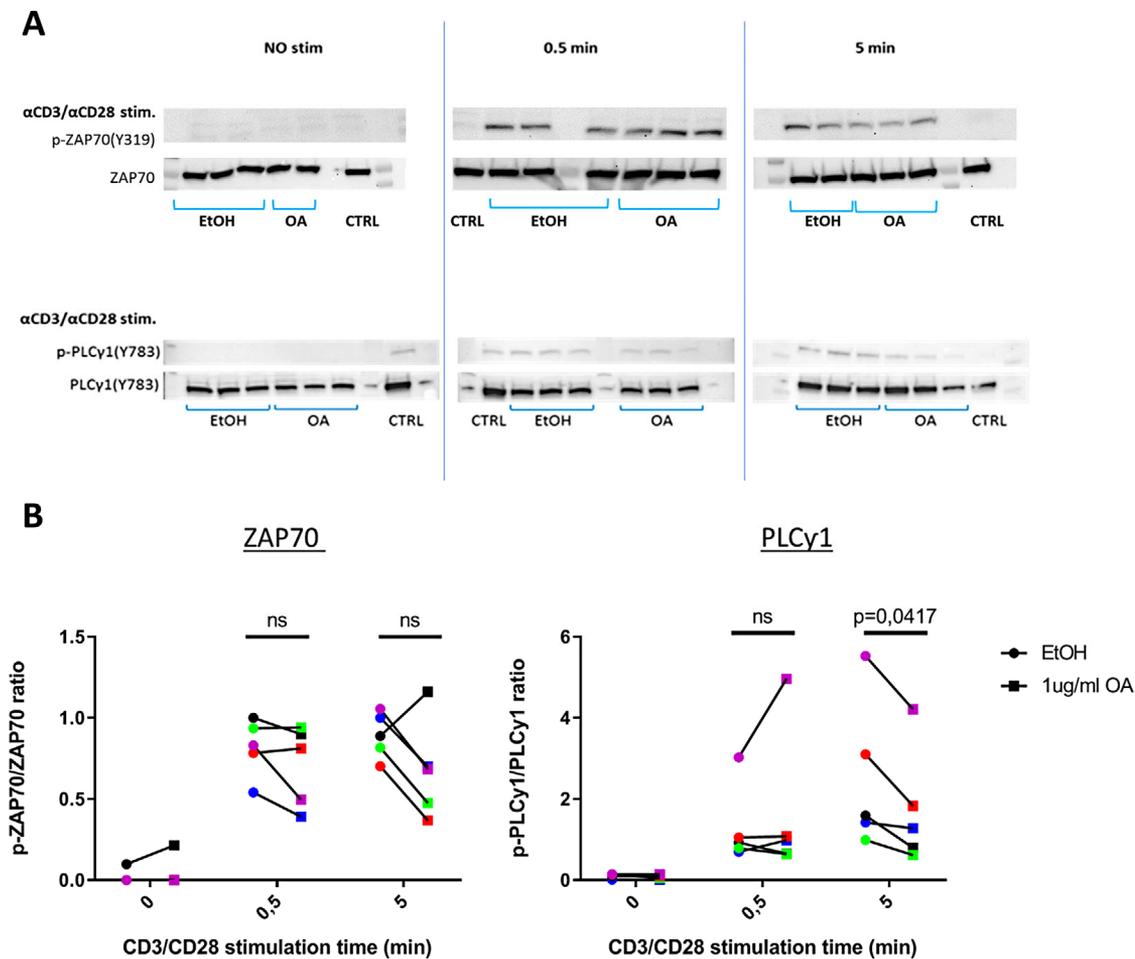
Figure 4. Early activation of TCR signaling events of CD3/CD28 activated CD4+ T cells incubated with oleic acid. (A) CD4+ T cells were treated with oleic acid (1 μg/mL) or solvent control and cells were harvested after 24 h, followed by incubation with plate-bound (pb) αCD3 and soluble (sol) αCD28 for 15 min. Stimulation was activated by crosslinking the antibodies by incubation with 5 μg/mL goat-α-mouse for 0.5 or 5 min. Blots of one representative donor for ZAP70/p-ZAP70(Y319) and PLCγ1/p-PLCγ1(Y783) are shown. CTRL = CD3/CD28 activated Jurkat cells, etOH = CD3/CD28 activated CD4+ T cells incubated with vehicle control, OA = CD3/CD28 activated CD4+ T cells incubated with oleic acid. (B) Summary of five different donors for ZAP70/p-ZAP70(Y319) and PLCγ1/p-PLCγ1(Y783). Data are shown as median from a triplicate of five different donors in five independent experiments. The signed rank test was performed ns >0.05.

via the calcineurin/NFAT pathway. This effect was mediated by an extracellular calcium influx via econazole-insensitive channels [29, 33]. In contrast, other studies have reported a reduced proliferation of Jurkat T [34] and lymphocytes as well as a reduction of the IL-2 response [35]. In the latter studies an anti-inflammatory response in T cells was suggested, using a much higher concentration (50–350 μM range) of oleic acid compared with our experiments (<35 μM). It has been previously reported that high concentrations of exogenous FA can induce apoptotic pathways and decreased cytokine production possibly explaining this apparent discrepancy [36].

Moreover, we also observed that, in contrast to 1 μg/mL oleic acid, which increased the IL-2 response, 10 μg/mL reduced the IL-2 response after 4 days. As IL-2 is both secreted and consumed by CD4+ T cells during activation and proliferation, our data could indicate that the balance between secretion and consumption might be skewed by oleic acid and this effect is dose-dependent. Alternatively, oleic acid could also affect proliferation in an IL-2-independent manner.

Our study indicates that oleic acid is incorporated into oleoyl-L-carnitine. Carnitine is present in the membrane of the mitochondria of primary CD4+ T cells and membrane UFA saturation levels are associated with altered Ca^{2+} uptake [37, 38]. Moreover, previous studies have shown that the accumulation of long-chain carnitines facilitates Ca^{2+} release from the sarcoplasmic reticulum [39]. We observed an accumulation of oleic acid in the mitochondria of the CD4+ T cells and this was paired by increased Ca^{2+} flux. Whether these two observations are causally linked remains to be determined.

Our results show a limited effect of oleic acid on CD4+ T-cell metabolism, as both glycolysis and oxidative phosphorylation (OXPHOS) were unaffected by the supplementation with oleic acid. These findings suggest that exogenous oleic acid is not used as an energy source. In previous publications, authors have found
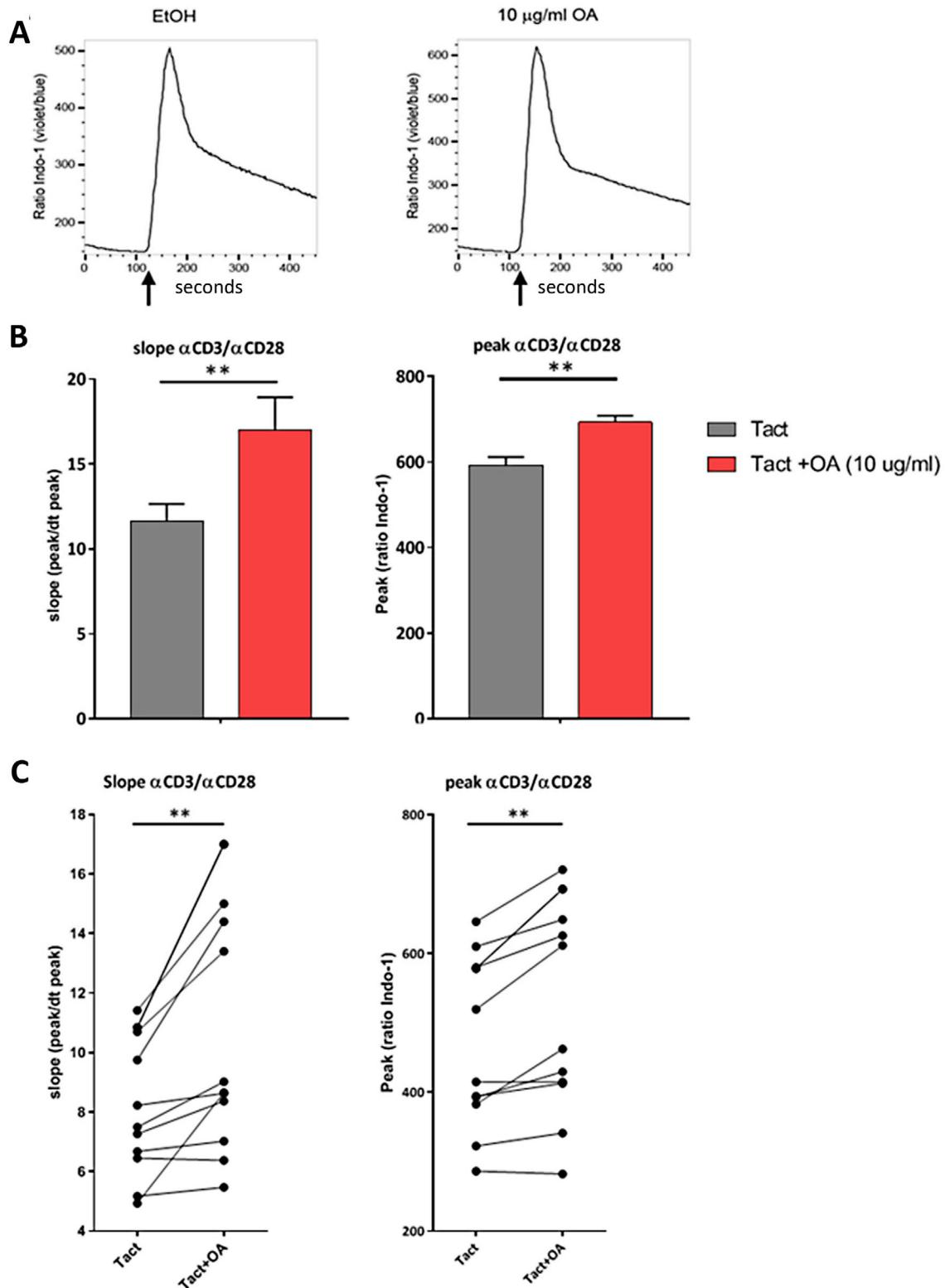
Figure 5. Calcium flux responses of CD3/CD28 activated CD4^{+} T cells incubated with oleic acid during the first 24 h. (A) CD4^{+} T cells were treated with oleic acid (10 μg/mL) or vehicle control (ethanol). After 24 h, cells were harvested and stained with indo-1 AM in the presence of plate-bound αCD3 and soluble αCD28. Calcium levels were measured for 2 min (basal levels) followed by crosslinking via the addition of 3 μg/mL goat-anti-mouse antibody (indicated by arrow) and calcium flux was measured for an additional 5 min. (A) A representative calcium flux plot is shown for both oleic acid (10 μg/mL) and vehicle control. The highest point of the peak and slope are shown. (B) Data are shown as mean + SD from quintuplets from one representative donor. A paired students *T*-test was performed. (C) Summary of 11 different donors is shown depicted are mean of quintuplets, a paired students *T*-test was performed **$p < 0.01$ in total in 11 independent experiments were performed.
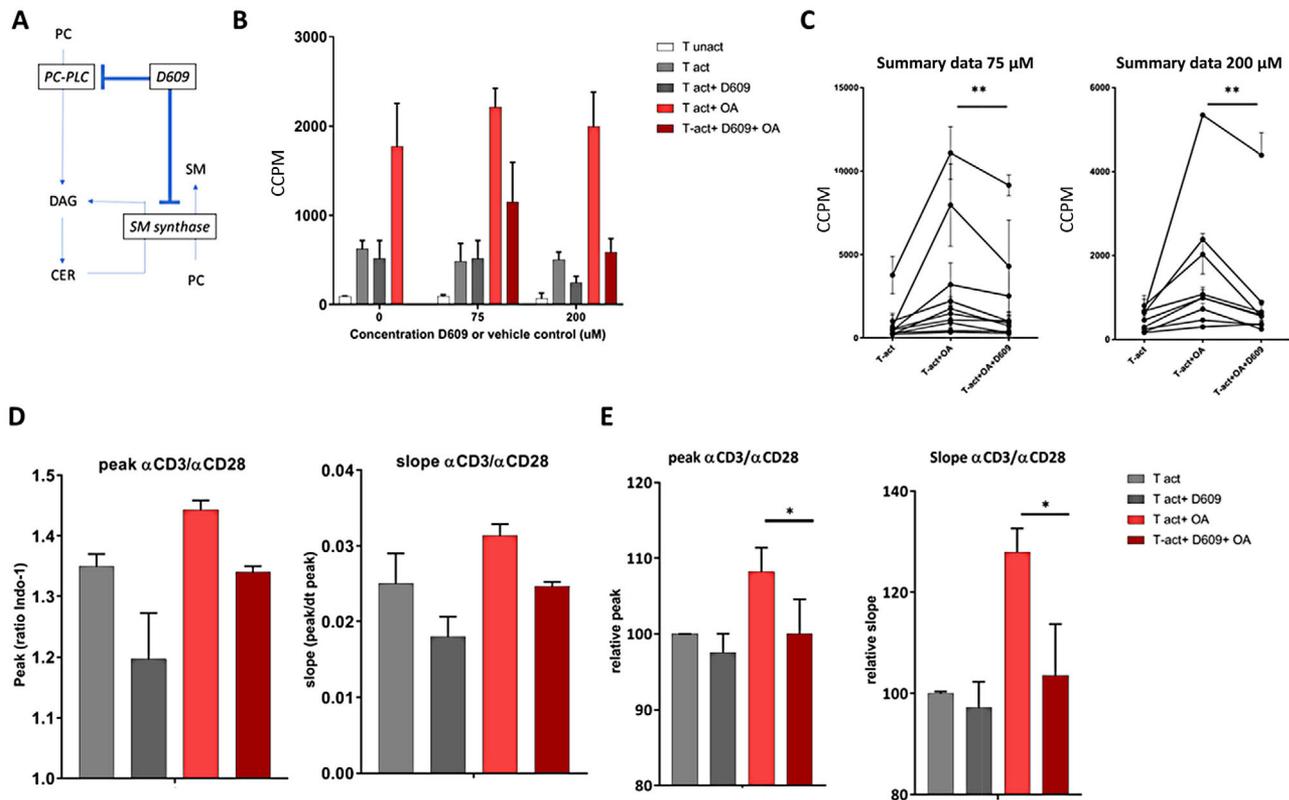
Figure 6. The effect on proliferation of the inhibition of sphingomyelin synthase by tricyclodecan-9-yl-xanthogenate (D609) on CD3/CD28 activated CD4$^+$ T cells incubated with oleic acid. (A) Schematic summary of inhibitory effect of D609, sphingomyelin synthase inhibitor on the synthesis of CER, ceramides; DAG, diacylglycerides; PC, phosphatidylcholine; and SM, sphingomyelin. (B) 1 h preincubation with inhibitor of phosphatidylcholine-specific phospholipase C (PC-PLC) D609 (75–200 μM), vehicle control (vehicle control contained Dimethyl sulfoxide instead of D609). The cells were treated for 24 h at 37°C. After 24 h, the medium was washed away and cells were labeled with 0.5 μCi 3H-thymidine and incubated with 1 μg/mL oleic acid (OA) or control, in the presence of plate-bound (pb) αCD3 and soluble (sol) αCD28 resuspended in fresh medium. The medium was removed after 24 h and cells were transferred to a new fresh medium in the presence of pb αCD3 and sol αCD28. Proliferation was measured after 3 days by lash and glow luminescence using a 1450 LSC & luminescence counter. Data are shown as mean + SD from sextuplo of one representative donor in a total of eight donors in eight independent experiments were performed, a paired students *T*-test was used. (C) Summary of the results of eight donors. Median + SEM were shown and a Wilcoxon signed-rank test was performed. (D) The peak and slope are shown of calcium flux. Data from one representative donor are shown as mean + SD of quintuplets. A student's *T*-test was performed (E) Relative change of the peak and slope of four different donors in independent experiments. A student's *T*-test was performed *$p < 0.05$, **$p < 0.01$. Ccpm = corrected count per minute

that exogenous FA does affect the glycolysis to OXPHOS ratio. However, these data were generated using poly-UFA instead of mono-UFA [40]. Differences with previous findings might also be due to the different CD4$^+$ T-cell subsets used. It has been reported that functional differentiation affects metabolic signature [14, 15, 38, 41] and the way cells process exogenous lipids [14, 42, 43]. Publications using settings similar to ours, found that UFA derived from extracellular sources were not directly used for FA oxidation but were instead produced in a cell-intrinsic manner via fatty acid synthesis [18]. Taken together, our data support previous data indicating that it is unlikely that exogenous oleic acid affects CD4$^+$ T cells through increased FA oxidation or other changes in metabolic signature.

In studies indicating an effect of exogenous UFA on TCR signaling it was suggested that the underlying mechanism was related to the disruption of the immunological synapse by increasing the concentration of unsaturated lipid species [9, 44]. TCR signaling results in the recruitment of different kinases and protein tyro-

sine phosphatases to the immunological synapse and oleic acid is known to affect the activity of such enzymes [45]. We have evaluated the effects of oleic acid on ZAP70 and PLCγ1 phosphorylation and found no significant changes at 30 s, while a decrease in PLCγ1 phosphorylation at the 5 min time point was observed in some donors (Fig. 5A). This apparent discrepancy could be due, among others, to differences in kinetics of the Ca^{2+} response vs kinase phosphorylation, or other direct or indirect effects of oleic on TCR-induced signaling pathways that result in enhanced T-cell proliferation. A better evaluation of the underlying causes would require more detailed measurements, which could be addressed in follow-up studies.

In concordance with our data, others have also found that UFA can directly induce the release of calcium from intracellular stores without the involvement of TCR membrane proteins [46, 47]. Further support that intracellular stores are involved is the observation that even in the absence of extracellular Ca^{2+}, the Ca^{2+} flux is positively affected by oleic acid. It was postulated that some UFA

can indeed directly bind Ca^{2+} channels via protein–lipid interactions or modify the properties of the membrane of intracellular Ca^{2+} stores.

In line with this hypothesis, we observed an effect of D609 on oleic acid-enhanced proliferation and calcium flux responses. D609 is widely used for SM synthase inhibition but it is also known to affect the synthesis of DAG [48]. TCR ligation leads to the hydrolysis of PIP2, generating DAG and free IP3, which subsequently causes the release of Ca^{2+} into the cytosol [49, 50]. The levels of PIP2 in the membrane are rapidly altered by the activity of phosphoinositide-directed kinases and phosphatases making it notoriously difficult to assess their dynamics correctly [51]. Due to the technical limitations and the dynamic nature of the PIP2, axis we did not quantify these signaling molecules ourselves and cannot draw definitive conclusions on whether the increase in calcium mobilization can be attributed to the saturation levels of PIP2. We did, however, detect increased levels of DAG 18:1 and PC 18:1 after oleic acid incubation suggesting that complex lipids containing oleic acid are increased. Furthermore, others have shown that an increase in FA with zero to two double bonds results in PIP2 saturation associated with enhanced T-cell proliferation [49]. Since we also observed an increase in DAG 18:1 in the presence of oleic acid and because DAG is an essential constituent of PIP2, it is conceivable that treatment with oleic acid results in PIP2 saturation. This could in turn result in an increase in calcium mobilization.

In conclusion, we uncovered that the incorporation of UFA into membrane lipids enhances the proliferation and Ca^{2+} mobilization in human primary $CD4^+$ T cells. In light of the technical difficulties regarding the identification of UFA interactions and the physical properties of lipid membranes, it is recommended that new tools have to be developed to study these mechanisms in more detail. Given the correlation between obesity and immune-related diseases, our findings might provide additional strategies to modulate T-cell-mediated responses via exogenous FA.

Materials and methods

$CD4^+$ T cells

These studies were conducted in a biosafety level 1 laboratory that relies on standard microbiological practices. Human peripheral blood mononuclear cells (PBMCs) were isolated from whole blood or from buffy coats of healthy volunteers (Sanquin) through Standard Ficoll density centrifugation. $CD4^+$ cells were isolated from the PBMCs by positive selection using Invitrogen Dynabead CD4 Positive Isolation Kit (Invitrogen, Dynal), according to the manufacturer's instructions. Briefly, Dynabeads were incubated with PBMCs, followed by magnetic separation of bead-bound cells. The positively isolated cells were then washed and the beads were detached. Purity was determined by FACS analysis. Cells were stained with antibody mixes containing the following surface markers: APC-conjugated CD4 (BD Biosciences), PE-conjugated CD3 (BD Biosciences)), FITC-conjugated CD8 (BD Biosciences), and PEcy7-conjugated CD14 (BD Biosciences). All antibodies were mouse-derived antibodies (all from BD Biosciences). Staining was performed at 4°C for 30 min in the dark. Afterward, cells were washed three times with PBS containing 2% sodium azide. Cells were then fixed in 4% paraformaldehyde (PFA). Samples were measured on LSR-II Flow Cytometry (BD Biosciences) and analyzed using BD Biosciences FACSDiva 8.0.2 (DIVA software).

T-cell stimulation

Isolated $CD4^+$ T cells were used fresh or from cryopreserved material stored in Dulbecco's Modified Eagle's Medium (Gibco) with 4500 mg/L D-glucose and L-glutamine, phenol red, 30% fetal bovine serum (FCS) (LUMC apothecary) and 10% dimethylsulfoxide. $CD4^+$ T cells were washed twice before they were cultured in Dulbecco's Modified Eagle's Medium (Gibco) with 4500 mg/L D-glucose and L-glutamine, phenol red, 10% FCS (LUMC apothecary), 100 U/mL Penicillin and streptomycin (LUMC apothecary), 2 mM GlutaMAX (LUMC apothecary), 50 IU IL-2 (Peprotech).For stimulation, 96-well round bottom plates (Corning or Greiner) were coated with 50 μL of 5 μg/mL anti-CD3 (clone OKT3, eBioscience) overnight at 4°C, followed by a wash with medium to remove the excess of CD3. Isolated $CD4^+$ T cells were added to the CD3-coated wells at a concentration of 100,000 cells/160 μL DMEM high glucose (4.5 g/L) with no sodium pyruvate (Sigma Aldrich supplemented with 100 U/mL penicillin and streptomycin, 2 mM GlutaMAX, 0.5% FFA free BSA (Sigma) containing 1 μg/mL anti-CD28 (Sanquin). Next, oleic acid diluted in EtOH was conjugated to fatty acid-free BSA by the addition of DMEM high glucose (4.5 g/L) with no sodium pyruvate, supplemented with 2% fatty-acid-free BSA, 100 U/mL penicillin/streptomycin, and 2 mM GlutaMAX, followed by two rounds of vortexing and sonication (30 s). Forty microliters of either medium, ethanol solvent control (Sigma), oleic acid (Sigma), or oleic acid(17-yne) (Avanti Lipids) was added to the T cells. The final ethanol concentration was below 0.1%. Cells were stimulated overnight at 37°C, then washed with PBS before further use. Cells were tested for viability using 200 nM DAPI. Counting beads (Beckman counter) were added to the cells before measurement to quantify the number of cells. The proportion of viable cells was determined by counting 20,000 cells on an LSR-II Flow Cytometer (BD). All conditions were performed in triplicate and viability was >95%.

Proliferation assay — 3H thymidine incorporation

$CD4^+$ T cells were stimulated in 96 round-bottom plates, in 200 μL medium according to the protocol described before. After 1 day of stimulation, the medium was removed. Cells were washed and resuspended cells were transferred to fresh CD3-coated wells. Proliferation was measured by pulsing these cells with 0.5 μCi 3H-thymidine (Thermo Fisher Scientific). Incorporation of 3H-thymidine was measured after 24 h or

was further incubated for another 3 days. Lash and glow luminescence were measured using a 1450 LSC & luminescence counter, Wallac Microbeta Trilux (Perkin Elmer). All measurements were performed in triplicate.

Proliferation Assay —— Cell trace violet staining

CD4$^+$ T cells were stimulated in 96 round-bottom plates, according to the protocol described before. CD4$^+$ T cells were labeled with 5 µM CTV (Life Technologies) in 1 mL of PBS/0.1%BSA at 37℃. After 15 min, cells were washed three times with cold 10% FCS/medium after which cells were resuspended in DMEM high glucose (4.5 g/L) with no sodium pyruvate, supplemented with 0.5% fatty acid-free BSA, 100 U/mL penicillin/streptomycin and 2 mM GlutaMAX and plated in a density of 100,000 cells/well in 200 µL medium in a 96-well plate. Cells were stimulated with 5 µg/mL plate-bound αCD3 and 1 µg/mL soluble αCD28 and treated with 0.1, 1, or 10 µg/mL oleic acid or solvent control. Cells were harvested and CTV dilution was measured after 24 h. Alternatively, cells were washed to remove oleic acid and further incubated for another 3 days, followed by measurement of CTV dilution on LSR-II Flow Cytometer (BD Biosciences) and Diva 6 software (BD Biosciences).

Receptor kinetics

CD4$^+$ T cells were stimulated as described above, in the presence of 10 µg/mL oleic acid or ethanol solvent control for 0,1,2,3,4,6, or24 h (final volume 200 µL, 100,000 cells/well). After the specified time, cells were washed with PBS + 0.5% BSA + 0.02% sodium azide and transferred to 96-well V bottom plates (Corning). After transfer, cells were either resuspended in PBS + 0.5%BSA + 0.02%sodium azide as a blank control or stained with a fluorescent antibody mix consisting of Alexa Fluor 488-conjugated TCRαβ (Biologend), Pacific Blue-conjugated CD3 (BD Biosciences), PE-CF 594 conjugated CD69 (BD Biosciences), Alexa Fluor 700-conjugated CD25 (Biolegend), or stained with a fluorescent isotype control mix IgG1 k Alexa Fluor 488(BD Biosciences), IgG1 k Pacific Blue (BD Biosciences), IgG1 k PE-CF 594(BD Biosciences), IgG1 k Alexa Fluor 700 (Biolegend). All antibodies were mouse-derived antibodies. Staining was performed at 4℃ for 30 min in the dark. Afterward, cells were washed three times with PBS containing 2% sodium azide. Cells were then fixed in 4% PFA and stored in the dark at 4℃ until further use, for a maximum of 1 week. Stained samples were measured on an LSR-II Flow Cytometer (BD Biosciences). All measurements were done in triplicate.

Lipid extraction and click chemistry

Lipid extraction was performed with 1.5×10^6 CD4$^+$ T cells. The cellular lipids were extracted by ice-cold CHCl$_3$/MeOH/NaCl (5:10:9, v/v/v). Cell pellets were first resuspended into 200 µL of 2% NaCl (w/v). Sequentially 500 µL MeOH, 250 µL CHCl$_3$, and 250 µL 2% NaCl (w/v) were added with vortexing between each step. The samples were vortexed for another 45 min. Samples were centrifuged at 14,000 rpm for 1 min. The lower organic phase containing the majority of cellular lipids were extracted with a Hamilton glass syringe. A second extraction was performed by adding 250 µL CHCl$_3$ to the aqueous upper phase. The extracts were combined and dried with a speed vacuum at medium speed for around 40 min. The lipid pellets were resuspended in 10 µL CHCl$_3$ and 64.5 µL coumarin click mixture containing 0.45 mM 3-azido-7-hydroxycoumarin (Carl Roth) and 1.45 mM Tetrakis(ACN)copper(I) tetrafluoroborate (Carl Roth) in acetonitrile/ethanol (3:7) solvent was added to perform the click reaction with oleic acid (17-yne). Samples were incubated for 2 h at 45℃ in the dark. Finally, the lipids were dried using a speed vacuum. Dried pellets were dissolved in 10 µL CHCl$_3$/MeOH (2:1, v/v) before thin layer chromatography separation. Coumarin fluorescence was visualized using a BIO-RAD Chemi-Doc XRS+ system.

Microscopy

CD4$^+$ T-cells were cultured and stimulated as described above. Cells were treated with 10 µg/mL oleic acid, 10 µg/mL oleic acid(17-yne), medium control, or ethanol solvent control. All conditions were measured in triplicate. Eight-well microscopy slides with removable chambers (Nunc Lab-Tek Chamber Slide system, Sigma) were coated with 250 µL/chamber of 50 µg/mL poly-D-lysine (LUMC apothecary) for 1 h. Next, the slides were washed twice with PBS and left to dry for 1 h. When the slides were dry, the T cells were transferred from the 96-well round bottom plate to the chambers and left to adhere for 1 h at 37℃, followed by fixation with 1% paraformaldehyde (LUMC Pharmacy) for 10 min to 1 h, followed by a wash with PBS.

Light microscopy

After fixating the cells, a click reaction was performed in the wells with Azide-fluor 488 - Azide fluor (AF488-azide). A mixture comprised of 1 mM copper sulfate (CuSO4, Sigma Aldrich), 0.5 µM (tris((1-((O-ethyl)carboxymethyl)-(1,2,3-triazol-4-yl))methyl)amine, 10 mM sodium ascorbate (Sigma Aldrich) and 2 µM of AF488-azide was prepared in PBS. Fifty microliters of the mixture was added to each well and left to react for 30 min at 4℃ in the dark. The cells were then washed once with 2 mM EDTA (Sigma) in PBS, 3% BSA (Sigma) in PBS, and three times with PBS. Finally, the chambers were removed, and the slides were covered with VECTASHIELD antifade mounting medium with DAPI (VECTOR laboratories) and covered with a 60 mm glass coverslip. The slides were then stored overnight at 4℃ in the dark to let the VECTASHIELD harden. Imaging was performed with a Nikon Eclipse E800 microscope.

Confocal microscopy

The preparation of the slides for the confocal microscopy was identical to light microscopy. Imaging was performed on the Broadband Confocal Leica TCS SP5, at 63× zoom. To stain mitochondria, cells were incubated for 30 min with 150 nM Mito Tracker Green FM (Molecular Probes) in the medium. All wells were checked with light microscopy (Nikon Eclipse E800) for abnormalities before imaging with confocal microscopy. Only oleic acid and oleic acid(17-yne) were fully imaged with the help of the confocal.

Electron Microscopy: CD4$^+$ T cells were cultured in 96-well round bottom plates (Corning or Greiner) at 500,000 cells/well. Culture medium was DMEM high glucose (4.5 g/L) with no sodium pyruvate (Sigma Aldrich supplemented with 100 U/mL Penicillin and streptomycin, 2 mM GlutaMAX, 0,5% free fatty acid (FFA) free BSA (Sigma) The 96-well round bottom plates were coated with 50 μl of 5 μg/mL anti-CD3 (eBioscience) overnight at 4°C. The cells were suspended in a concentration of 500,000 cells/80 μL in a medium containing 1 μg/mL anti-CD28 (Sanquin). The anti-CD3 coated plates were washed with PBS to remove excess anti-CD3 and 160 μl of the cell and anti-CD28 mixture was added. Afterward, 40 μL of 10 μg/mL oleic acid or 40 μL of 10 μg/mL oleic acid(17-yne) was added. A total of 20 × 10^6 cells per condition was used to generate a pellet of adequate size for further treatment. After overnight incubation at 37°C, the cells were washed twice with 0.1 M PHEM buffer (Sigma). The cells were resuspended in 100 μL 0.1 M PHEM buffer and 100 μL of 0.2 M PHEM buffer to which 8% PFA was added. The cells were then left overnight at RT. The following day they were washed twice with 0.1 M PHEM buffer. The click reaction was performed next. A mixture comprised of 1 mM copper sulfate (CuSO4, Sigma), 0.5 μM tris((1-((O-ethyl)carboxymethyl)-(1,2,3-triazol-4-yl))methyl)amine, 10 mM sodium ascorbate (Sigma), and 2 μM of AF488-azide was prepared in PBS. Fifty microliters of the mixture was added to each well and left to react for 30 min in the dark at 4°C. The cells were washed once with 2 mM EDTA in PBS, 3% BSA in PBS, and three times with PHEM buffer. The cells were transferred from the 96-well round bottom plates to 2 ml Eppendorf tubes. After transfer, the cells were fixed for 2 h in 0.2% glutaraldehyde (EMS) and 2% paraformaldehyde (EMS) in PHEM buffer. After the glutaraldehyde fixation the cells were embedded in 12% gelatine (Sigma) in phosphate buffer, infiltrated in 2.3 M sucrose (Sigma) in phosphate buffer, and plunged in liquid nitrogen. Ultrathin sections were cut from the frozen cells using a cryoultramicrotome (Leica) equipped with a diamond knife (Diatome). The cryosections were transferred to a formvar- and carbon-coated copper grid. The sections attached to the grid were rinsed to remove the gelatin and sucrose. For imaging in the light microscope, the immunolabelled sections were stained with DAPI (Sigma-Aldrich) and embedded in 1.8% methylcellulose and air-dried (25 cP, Sigma-Aldrich) after which the grid with the sections were mounted on a glass slide in 50% glycerol and imaged in a CSLM (Leica, TCS, SP8) equipped with a 63× oil immersion objective (N.A. = 1.4). After imaging in the light microscope, the grid with the sections was removed from the glass slide and rinsed in water. The sections were then embedded in 1.8% methylcellulose and 0.6% Uranyl acetate and air-dried and imaged in a Tecnai12 Biotwin transmission electron microscope (FEI Company) operating at 120 kV, equipped with an Eagle 4kx4k CCD camera. Using stitching software, montages of 10 × 10 images at 11,000× were generated to retrace regions of interest identified in the light microscope. Superimposition and correlation of light and electron microscopy images were performed using Photoshop. All conditions were performed with single measurements. An activation control was taken along, at 100,000 cells/well. Before and after overnight fixation the cells were stained with anti-CD25 Alexa Fluor 700 and the staining was measured on an LSR-II Flow Cytometer (BD Biosciences).

T-cell metabolomics

Unstimulated or 5 μg/mL plate-bound αCD3 and 1 μg/mL soluble αCD28 stimulated cells were plated in 200 μL DMEM high glucose (4.5 g/L) with no sodium pyruvate, supplemented with 0.5% fatty-acid free BSA, 100 U/mL penicillin/streptomycin and 2 mM GlutaMAX in a density of 300,000 cells/well in a 96-well plate and treated with 0.1, 1, or 10 μg/mL oleic acid or 0.1, 1, or 10 μg/mL U13C oleic acid. After 8 and 24 h, cells (1.2 × 10^6 cells) from four wells per condition were pooled and washed with ice-cold PBS and metabolites were extracted in 50 μL lysis buffer containing methanol/acetonitrile/dH2O (2:2:1). Samples of medium cultured for 8 and 24 h were also collected. One milliliter of lysis buffer was added to 10 μL of medium to extract metabolites. Samples were centrifuged at 16,000g for 15 min at 4°C. Supernatants were collected for LC-MS analysis.

T-cell metabolism-Seahorse

Purified peripheral blood CD4$^+$ T cells were plated in 50 μg/mL poly-D-lysine (Millipore) coated XF-plates (Seahorse) in a density of 300,000 cells/well in 160 μL XF media (non-buffered DMEM high glucose (4.5 g/L) with no sodium pyruvate (Sigma Aldrich, Germany), supplemented with 0.5% fatty-acid-free BSA, 100 U/mL penicillin/streptomycin and 2 mM GlutaMAX). Cells were incubated for 1 h in a non-CO$_2$ incubator. Prior to measurement of the OCR and ECAR 40 μL of 0.1 μg/mL, 1 μg/Ml, or 10 μg/ml oleic acid or solvent control was added. Basal OCR and ECAR levels were measured as well as levels after injection of 300,000 Dynabeads Human T-Activator CD3/CD28 (Invitrogen) using an XF-96 Flux analyzer (Seahorse Bioscience). In addition, unstimulated or 5 μg/mL plate-bound αCD3 and 1 μg/mL soluble αCD28 stimulated CD4$^+$ T cells were pretreated for 24 h with oleic acid after which cells were transferred to poly-D-lysine coated XF-plates (Seahorse) and incubated for 1 h in a non-CO$_2$ incubator after which basal OCR and ECAR levels were measured.

Western blots

Isolated CD4$^+$ T cells or Jurkat (E6.1) cells were plated in a six-well plate with a density of 2.5×10^6 cells/well in DMEM (Gibco) with 4500 mg/L D-glucose and L-glutamine, 100 U/mL Penicillin and Streptomycin, 2 mM GlutaMAX, 2% FFA free BSA. Cells were treated by adding 10 µg/mL oleic acid or the EtOH control to the cells and incubated for 24 h at 37°C. A total of 4×10^6 cells for each condition were harvested and resuspended at 10×10^6 cells/mL in the medium. Cells were stimulated in 400 µL for each condition. Stimulation was performed by incubation with 5 µL/mL anti-CD3 and 1 µg/mL anti-CD28 for 15 min followed by cross-linking with 5 µg/mL goat-anti mouse IgG-HRP (DAKO) for 0.5 min or 5 min at 37°C. Signaling was stopped by the addition of 1 mL ice-cold PBS.

The stimulated CD4$^+$ T cells and Jurkat cells (control) were lysed on ice for 1 h in 30 µl NP-40 lysis buffer (Invitrogen) in the presence of 1:100 phosphatase/protease inhibitor (Cell signaling) while vortexing every 15 min. Lysates were centrifuged at 4°C for 15 min at 14,000 rpm. Supernatants were stored at −80 C until further analysis. The protein content of the cell lysates was measured using the PierceTM BCA Protein Assay Kit (Pierce). The absorbance was measured with SpectraMax i3X and analyzed with Softmax Pro. SDS electrophoresis was performed using standard procedures. Ten micrograms of protein was diluted with 4× Laemmli sample buffer (BioRad)/5% β-mercaptoethanol (Merck) and boiled for 5 min at 95°C. Proteins were separated by SDS/PAGE on a 10-slot TGX mini-protean precast 7.5% gel (BioRad) followed by protein transfer on a Trans-Blot Turbo Transfer pack (BioRad). The membrane was washed and blocked with tris-buffered saline (TBS) (pH 7.6)/0.1% Tween/5% skim milk powder (Sigma Aldrich) for 1 h at RT under continuous rolling. Next, the membrane was incubated with 1:1000 phospho-PLCy1(Tyr783) rabbit antibody (P0448) in TBS/0.1%Tween/5%milk or PLC-y1 (Cell Signaling) or P-ZAP70(Tyr319) (Cell Signaling, 2701S) or ZAP-70 (Cell Signaling) in TBS/0.1%Tween/5%BSA overnight at 4°C. The membrane was washed and incubated with 1:5000 goat anti-rabbit Ig-HRP antibody (DAKO) in TBS/0.1%Tween/5%milk for 1 h at RT after which the membrane was washed with TBS/0.1% Tween and miliQ water. Stripping of the antibodies from the blot between the antibodies was performed by incubating in Stripping buffer (ThermoFisher Scientific) for 25 min 37°C, followed by six times washing for 5 min at RT and blocking for 1 h. Antigen capture was visualized using an enhanced chemiluminescence solution. The bands were measured by their chemiluminescence (BioRad Imaging System Chemic). The blot before overexposure was chosen for analysis. Quantitative analysis of the bands was performed with the IMAGE Lab 5.2 Program. Reference bands were chosen for each blot and the relative intensities of the other bands were determined for p-PLCy1 and PLCy1. The ratio of p-PLCy1 over the corresponding PLCy1 band was calculated as a measure of PLCy1 activity.

Calcium flux measurements

Purified CD4$^+$ T cells were incubated with 10 µg/mL oleic acid or EtOH in a density of 3×10^6 cells/well in 2.5 mL DMEM high glucose (4.5 g/L) with no sodium pyruvate, supplemented with 0.5% fatty-acid-free BSA, 100 U/mL penicillin/streptomycin, and 2 mM GlutaMAX in a six-well plate. After 24 h, cells were harvested and 2×10^6 were stained for 35 min at 37°C with 2 µM Indo-1 acetoxymethyl ester (Indo-1 AM) (Thermo Fisher Scientific) in 0.2 mL DMEM high glucose (4.5 g/L) with no sodium pyruvate, supplemented with 2% fatty-acid-free BSA in the presence of 0.02% pluronic acid and 5 µg/mL αCD3 and 1 µg/mL αCD28. Cells were washed and taken up in 1 mL DMEM high glucose (4.5 g/L) with no sodium pyruvate, supplemented with 2% FFA-free BSA and 1 mM CaCl$_2$. In the experiments where extracellular calcium was depleted, DMEM high glucose (4.5 g/L) with no sodium pyruvate, supplemented with 2% FFA-free BSA and 2 mM Chelator EGTA (Sigma E4378) was used. Next, cells were warmed up to 37°C in a water bath, and baseline calcium flux was measured on an LSR-II Flow Cytometer (BD Biosciences) for 2 min before the addition of 3 µg/mL goat-anti-mouse antibody (Dako) to cross-link αCD3 and αCD28 after which calcium flux was measured for an additional 5 min.

Cytokine and transcription factor measurements

CD4$^+$ T cells were stimulated with plate-bound αCD3 and soluble αCD28 in the presence of oleic acid (1–10 µg/mL) or vehicle control. Stimulation and culture were performed as described before but cultures were in the absence of IL-2 supplementation. IL-2 production was assessed in the supernatant of these cultures with Human IL-2 ELISA MAX Deluxe (Biolegend). Other cytokines, IFN-γ, IL-10, IL-4, IL-5, IL-6, and TNF-α were measured in supernatant of CD4$^+$ T cells using the Milliplex Human Th17 Magnetic BeadPanel (Millipore), the Bio-Plex array reader and Bio-Plex software, according to manufacturer's protocol.

Inhibition proliferation assay

For the inhibition experiments, oleic acid was added after 1 h preincubation with an inhibitor of phosphatidylcholine-specific phospholipase C tricyclodecan-9-yl-xanthogenate (D609), or DMSO control. DMEM supplemented with 2% FFA-free BSA was used to dilute D609 to its desired concentrations. With final concentrations of 100,000 or 500,000 cells/well in 200 µL with 1 µg/mL anti-CD28. The cells were treated for 24 h at 37°C, followed by resuspension in fresh medium. Proliferation, calcium flux, or lipid extraction were performed as described.

Lipid analysis

Different acquisition and quantification methods were performed using different mass spectrometer systems throughout this manuscript. Differential mobility electrospray ionization, tandem mass spectrometry (DMS-ESI($\pm$)MS/MS) Lipidyzer, Fourier transform ion cyclotron resonance mass spectrometry (LC-FT/MS), and two methods based on liquid chromatography-tandem mass spectrometry (LC/MS/MS) were performed to acquire the data described in this manuscript. Samples were acquired as described previously in this Materials and Methods section and injected into their respective mass spectrometer systems.

DMS-ESI($\pm$)MS/MS (Lipidyzer)

Acquisition and quantification were performed using the Lipidyzer platform, consisting of a QTrap 5500 mass spectrometer (Sciex) with differential ion mobility spectrometry, coupled to a Shimadzu Nexera X2 LC system, for flow injection, and the Lipidomics workflow manager software. A detailed description of the quantitation process can be found in references [52, 53]. Briefly, the resuspended sample was injected twice using a Shimadzu SIL 30AC autosampler into a running buffer consisting of 10 mM ammonium acetate in 50:50 (v/v) dichloromethane:methanol at a flow rate of 7 μL/min. Two different methods were applied. Method #1 operated with active DMS separation under the following conditions, DMS temperature low, modifier (propanol) composition low, separation voltage 3500 V, DMS resolution enhancement low. Method #2. The MS operated under the following conditions: curtain gas 17, CAD gas medium, ion spray voltage 4100 V in ESI$^+$ mode and -2500 V in ESI$^-$ mode, temperature 200°C, nebulizing gas 17, and heater gas 25. Quantification of lipid species was achieved by internal calibration using several deuterated internal standards (IS) (Sciex cat# 504156) for each lipid class within the lipidomics workflow manager. Each lipid species is corrected by the closest deuterated IS within its lipid class, in terms of carbon and double bond number of the fatty acid side chain. Subsequently, the obtained area ratio is multiplied by the concentration of the respective IS and corrected for volume and weight; as a consequence, this quantitation can be considered accurate within a specified quantitative bias. The following 13 lipid classes were quantitatively assessed: CE, cholesterol ester; CER, ceramides; DAG, diacylglycerides; DCER, dihydroceramides; FFA, free fatty acids; HCER, hexosylceramides; LPC, lysophosphatidylcholine; LPE, lysophosphatidylethanolamine; PC, phosphatidylcholine; PE, phosphatidylethanolamine; SM, sphingomyelin; and TAG, triacyltriglycerides.

Lipid analysis (LC-FT/MS)

Both cell and medium samples were analyzed on the LC-FT/MS. 750.000 cells were resuspended in 20 μL PBS (pH 7.4 [-] CaCl2, [-] MgCl2) and transferred into 295 μL of isopropanol in a 1.5 mL Eppendorf tube, then the remainder of cells were resuspended in 10 μL PBS (pH 7.4 [-] CaCl2, [-] MgCl2) and transferred into the isopropanol. For calibration range samples 30 μL PBS (pH 7.4 [-] CaCl2, [-] MgCl2) and for medium samples 30 μL of the medium was added to 290 (calibration range samples) or 295 μL (medium samples) isopropanol. Then 5 μL of an internal standard containing ergosterol acetate, LPC (19:0), PC (11:0/11:0), PE (15:0/15:0), and TG (17:0/17:0/17:0) in isopropanol was added. The final concentration, the concentration to be analyzed on the LC-FT/MS, of these lipids was 0.1 μg/mL except for ergosterol acetate whose final concentration was 1 μg/mL. The samples were sonicated for 5 min and centrifuged (16.100 rcf, 5 min.; Eppendorf 5415R). Finally, 100 μL of supernatant was complemented with 100 μL water and put into an Agilent auto-sampler vial with a glass insert. Samples were measured immediately or stored at -80°C until analysis.

Lipids were analyzed using a Dionex Ultimate 3000 LC-system coupled to a 12T Bruker solariX XR mass spectrometer. Ten microliters of the sample was injected and separated on a phenomenex kinetex 1.7 μm, c18 (50 $\times$ 2.1 mm; 100 Å) column, which was held at 50°C. The mobile phase flow rate was 250 μL/mL and a gradient of eluent A (80% water, 20% acetonitrile, 5 mM ammonium formate, and 0.05% formic acid) and B (90% isopropanol, 9% acetonitrile, 1% water, 5 mM ammonium formate, and 0.05% formic acid) was used to elute the lipids from the column. The gradient was programmed as follows: 0–1 min. 50% B, 1–8 min. linear increase to 95% B, 8–10 min. stable at 95% B, 10–10.5 min linear decrease to 50% B, and 10.5–15 min stable at 50% B. A post-column flow splitter was used. Compounds were ionized using electron spray ionization. N2 was used as a nebulizer (1.3 bar) and drying gas (4.0 L/min.), and the dry temperature of the source was set at 200°C. The capillary voltage was 4300 V. Compounds were detected in the positive mode, and m/z-values between 200 and 1200 were detected.

Data analysis of masses in the spectra of LC-FT/MS data were internally calibrated using the monoisotopic mass of LPC (19:0), PC (11:0/11:0), PE (15:0/15:0) and TG (17:0/17:0/17:0). Extracted Ion Chromatograms of the compounds to be quantified were formed. PCs and TGs were quantified using an external calibration curve of PC (19:0/19:0) and TG (15:0/15:0/15:0), respectively. For the quantitation of PCs PC(11:0/11:0) and TGs TG (17:0/17:0/17:0) was used as internal standard. Linear calibration curves were weighted using a weight factor of two on the concentration [54].

Lipid analysis (LC/MS/MS)

Individual lipid classes and neutral lipids were separated by thin-layer chromatography (TLC) on silica gel-60G plates, 5 $\times$ 10 cm (Merck), using CHCl3/MeOH/H2O (60:25:4, v/v/v). The lipids containing oleic acid(17-yne) were visualized with UV light via the coumarin fluorophore. Visible bands were scraped off, and collected in Eppendorf tubes. Bands from the oleic acid-treated

T cells were also scraped off at the same height. Lipids were extracted from the silica two times 750 µL DCM/MeOH (2:1). Lipids samples were stored at –80°C before further analysis. Lipid classes were classified by LC/MS/MS (Sciex TripleTOF 6600) with an injection volume of 10 µL. Before injection, lipids were dried with nitrogen and redissolved in isopropanol/water (1:1) with a sonication of 30 sec. The data was analyzed using Lipid Data Analyzer.

LC-MS analysis was performed on an Exactive mass spectrometer (Thermo Fisher Scientific) coupled to a Dionex Ultimate 3000 autosampler and pump (Thermo Fisher Scientific). The MS operated in polarity-switching mode with a spray voltage of 4.5kV and −3.5 kV. metabolites were separated using a Sequant ZIC-pHILIC column (2.1 × 150 mm, 5 µm, guard column 2.1 × 20 mm, 5 µm; Merk) using a linear gradient of acetonitrile and eluent A (20mM $(NH_4)_2CO_3$,0.1% NH_4OH in ULC/MS grade water (Biosolve)) Flow rate was set at 150 µL/min. Metabolites were identified and quantified using LCquan software (Thermo Fisher Scientific) on the basis of exact mass within 10 ppm and further validated by concordance with retention times of standards. Peak intensities were normalized based on total ion count.

Statistics

Statistical analyses were performed using GraphPad Prism 7.02 (GraphPad Software Inc). A paired students *T*-test was performed when the data was normally distributed (Kolmogorov–Smirnov test >0.05)), and data were shown in mean + SD. Wilcoxon Signed Rank Test was performed when the data was not normally distributed (Kolmogorov–Smirnov test < 0.05), data was shown in median + SEM. Asterisks indicate a significant effect of treatment compared with controls. *$P < 0.05$; **$P < 0.01$; ***$P < 0.001$.

Conflict of interest: The authors declare no commercial or financial conflict of interest.

Author contributions: von Hegedus wrote the original draft of the manuscript. Ioan-Facsinay conceived the project, supervised the research study, and designed experiments. von Hegedus, de Jong, Spronsen Zhu, Cabukusta, Kwekkeboom, Heijink, and Hoekstra conducted experiments and collected data. Ioan-Facsinay and Toes provided resources. Giera, Bos, and Berkers contributed to the methodology. All authors provided a discussion and agreed to the final version.

Data availability statement: The authors confirm that the data supporting the findings of this study are available within the article and its supplementary materials. Additional data that was generated during the experiments described in this article are available upon reasonable request.

Peer review: The peer review history for this article is available at https://publons.com/publon/10.1002/eji.202350685.

References

1 Jain, A., Irizarry-Caro, R. A., McDaniel, M. M., Chawla, A. S., Carroll, K. R., Overcast, G. R., Philip, N. H. et al., T cells instruct myeloid cells to produce inflammasome-independent IL-1β and cause autoimmunity. *Nat. Immunol.* 2020. **21**: 65–74.

2 Tan, H., Yang, K., Li, Y., Shaw, T. I., Wang, Y., Blanco, D. B., Wang, X., et al. Integrative proteomics and phosphoproteomics profiling reveals dynamic signaling networks and bioenergetics pathways underlying T cell activation. *Immunity* 2017. **46**: 488–503. This study shows that mTORC1 remodels mitochondrial metabolism and glycolysis through regulation of the T cell proteome and phosphoproteome.

3 Menk, A. V., Scharping, N. E., Moreci, R. S., Zeng, X., Guy, C., Salvatore, S., Bae, H. et al., Early TCR signaling induces rapid aerobic glycolysis enabling distinct acute T cell effector functions. *Cell Rep.* 2018. **22**: 1509–1521.

4 Sinclair, L. V., Rolf, J., Emslie, E., Shi, Y. B., Taylor, P. M. and Cantrell, D. A., Control of amino-acid transport by antigen receptors coordinates the metabolic reprogramming essential for T cell differentiation [published correction appears in Nat Immunol. 2014 Jan;15(1):109]. *Nat. Immunol.* 2013. **14**: 500–508.

5 Niinistö, S., Takkinen, H. M., Erlund, I., Ahonen, S., Toppari, J., Ilonen, J., Veijola, R. et al., Fatty acid status in infancy is associated with the risk of type 1 diabetes-associated autoimmunity. *Diabetologia* 2017. **60**: 1223–1233.

6 Scoville, E. A., Allaman, M. M., Adams, D. W., Motley, A. K., Peyton, S. C., Ferguson, S. L., Horst, S. N. et al., Serum polyunsaturated fatty acids correlate with serum cytokines and clinical disease activity in Crohn's disease. *Sci. Rep.* 2019. **9**: 2882.

7 Meessen, J., Saberi-Hosnijeh, F., Bomer, N., den Hollander, W., van der Bom, J. G., van Hilten, J. A., van Spil, W. E. et al., Serum fatty acid chain length associates with prevalent symptomatic end-stage osteoarthritis, independent of BMI. *Sci. Rep.* 2020. **10**: 15459.

8 Han, S. N., Lichtenstein, A. H., Ausman, L. M. and Meydani, S. N., Novel soybean oils differing in fatty acid composition alter immune functions of moderately hypercholesterolemic older adults. *J. Nutr.* 2012. **142**: 2182–2187.

9 Arcaro, A., Grégoire, C., Boucheron, N., Stotz, S., Palmer, E., Malissen, B. and Luescher, I. F., Essential role of CD8 palmitoylation in CD8 coreceptor function. *J. Immunol.* 2000. **165**: 2068–2076.

10 Geyeregger, R., Zeyda, M., Zlabinger, G. J., Waldhäusl, W. and Stulnig, T. M., Polyunsaturated fatty acids interfere with formation of the immunological synapse. *J Leukoc Biol* 2005. **77**: 680–688.

11 Larbi, A., Grenier, A., Frisch, F., Douziech, N., Fortin, C., Carpentier, A. C. and Fülöp, T., Acute in vivo elevation of intravascular triacylglycerol lipolysis impairs peripheral T cell activation in humans. *Am. J. Clin. Nutr.* 2005. **82**: 949–956.

12 Kidani, Y., Elsaesser, H., Hock, M. B., Vergnes, L., Williams, K. J., Argus, J. P., Marbois, B. N. et al., Sterol regulatory element-binding proteins are

essential for the metabolic programming of effector T cells and adaptive immunity. *Nat. Immunol.* 2013. **14**: 489–499.

13 **Cluxton, D., Petrasca, A., Moran, B. and Fletcher, J. M.**, Differential regulation of human Treg and Th17 cells by fatty acid synthesis and glycolysis. *Front. Immunol.* 2019. **10**: 115.

14 **Wang, R., Dillon, C. P., Shi, L. Z., Milasta, S., Carter, R., Finkelstein, D., McCormick, L. L. et al.**, The transcription factor Myc controls metabolic reprogramming upon T lymphocyte activation. *Immunity* 2011. **35**: 871–882.

15 **Wang, R. and Green, D. R.**, Metabolic checkpoints in activated T cells. *Nat. Immunol.* 2012. **13**: 907–915.

16 **Michalek, R. D., Gerriets, V. A., Jacobs, S. R., Macintyre, A. N., MacIver, N. J., Mason, E. F., Sullivan, S. A. et al.**, Cutting edge: distinct glycolytic and lipid oxidative metabolic programs are essential for effector and regulatory CD4+ T cell subsets. *J. Immunol.* 2011. **186**: 3299–3303.

17 **Pacella, I., Procaccini, C., Focaccetti, C., Miacci, S., Timperi, E., Faicchia, D., Severa, M. et al.**, Fatty acid metabolism complements glycolysis in the selective regulatory T cell expansion during tumor growth. *Proc. Natl. Acad. Sci. USA* 2018. **115**: E6546–E6555.

18 **O'Sullivan, D., van der Windt, G. J., Huang, S. C., Curtis, J. D., Chang, C. H., Buck, M. D., Qiu, J. et al.**, Memory CD8(+) T cells use cell-intrinsic lipolysis to support the metabolic programming necessary for development. *Immunity* 2014. **41**: 75–88.

19 **Pan, Y., Tian, T., Park, C. O., Lofftus, S. Y., Mei, S., Liu, X., Luo, C. et al.**, Survival of tissue-resident memory T cells requires exogenous lipid uptake and metabolism. *Nature* 2017. **543**: 252–256.

20 **Furuhashi, M. and Hotamisligil, G. S.**, Fatty acid-binding proteins: role in metabolic diseases and potential as drug targets. *Nat. Rev. Drug Discov.* 2008. **7**: 489–503.

21 **Muroski, M. E., Miska, J., Chang, A. L., Zhang, P., Rashidi, A., Moore, H., Lopez-Rosas, A. et al.**, Fatty acid uptake in T cell subsets using a quantum dot fatty acid conjugate. *Sci. Rep.* 2017. **7**: 5790.

22 **Staiger, H., Staiger, K., Stefan, N., Wahl, H. G., Machicao, F., Kellerer, M. and Häring, H. U.**, Palmitate-induced interleukin-6 expression in human coronary artery endothelial cells. *Diabetes* 2004. **53**: 3209–3216.

23 **Mustonen, A. M., Käkelä, R., Lehenkari, P., Huhtakangas, J., Turunen, S., Joukainen, A., Kääriäinen, T. et al.**, Distinct fatty acid signatures in infrapatellar fat pad and synovial fluid of patients with osteoarthritis versus rheumatoid arthritis. *Arthritis Res. Ther.* 2019. **21**: 124.

24 **Tutunchi, H., Ostadrahimi, A. and Saghafi-Asl, M.**, The effects of diets enriched in monounsaturated oleic acid on the management and prevention of obesity: a systematic review of human intervention studies. *Adv. Nutr.* 2020. **11**: 864–877.

25 **Ioan-Facsinay, A., Kwekkeboom, J. C., Westhoff, S., Giera, M., Rombouts, Y., van Harmelen, V., Huizinga, T. W. et al.**, Adipocyte-derived lipids modulate CD4+ T-cell function. *Eur. J. Immunol.* 2013. **43**: 1578–1587.

26 **Cucchi, D., Camacho-Muñoz, D., Certo, M., Pucino, V., Nicolaou, A. and Mauro, C.**, Fatty acids - from energy substrates to key regulators of cell survival, proliferation and effector function. *Cell Stress* 2019. **4**: 9–23.

27 **Medrano, M., Lemus-Conejo, A., Lopez, S., Millan-Linares, M. C., Rosillo, M. A., Muñiz, M., Calderon, R. et al.**, CD4+ and CD8+ T-cell responses in bone marrow to fatty acids in high-fat diets. *J. Nutr. Biochem.* 2022. **107**: 109057.

28 **Wall, R., Ross, R. P., Fitzgerald, G. F. and Stanton, C.**, Fatty acids from fish: the anti-inflammatory potential of long-chain omega-3 fatty acids. *Nutr. Rev.* 2010. **68**: 280–289.

29 **Gorjão, R., Cury-Boaventura, M. F., de Lima, T. M. and Curi, R.**, Regulation of human lymphocyte proliferation by fatty acids. *Cell Biochem. Funct.* 2007. **25**: 305–315.

30 **Zurier, R. B., Rossetti, R. G., Seiler, C. M. and Laposata, M.**, Human peripheral blood T lymphocyte proliferation after activation of the T cell receptor: effects of unsaturated fatty acids. *Prostaglandins Leukot. Essent. Fatty Acids* 1999. **60**: 371–375.

31 **Hein, C. D., Liu, X. M. and Wang, D.**, Click chemistry, a powerful tool for pharmaceutical sciences. *Pharm. Res.* 2008. **25**: 2216–2230.

32 **Gaebler, A., Milan, R., Straub, L., Hoelper, D., Kuerschner, L. and Thiele, C.**, Alkyne lipids as substrates for click chemistry-based in vitro enzymatic assays. *J. Lipid Res.* 2013. **54**: 2282–2290.

33 **Carrillo, C., Giraldo, M., Cavia, M. M. and Alonso-Torre, S. R.**, Effect of oleic acid on store-operated calcium entry in immune-competent cells. *Eur. J. Nutr.* 2017. **56**: 1077–1084.

34 **Verlengia, R., Gorjão, R., Kanunfre, C. C., Bordin, S., de Lima, T. M. and Curi, R.**, Effect of arachidonic acid on proliferation, cytokines production and pleiotropic genes expression in Jurkat cells–a comparison with oleic acid. *Life Sci.* 2003. **73**: 2939–2951.

35 **Yaqoob, P. and Calder, P. C.**, The effect of dietary lipid manipulation on the production of murine T-cell derived cytokines. *Biochem. Soc. Trans.* 1995. **23**: 279S.

36 **Zhu, Y., Schwarz, S., Ahlemeyer, B., Grzeschik, S., Klumpp, S. and Krieglstein, J.**, Oleic acid causes apoptosis and dephosphorylates Bad. *Neurochem. Int.* 2005. **46**: 127–135.

37 **Yog, R., Barhoumi, R., McMurray, D. N. and Chapkin, R. S.**, n-3 polyunsaturated fatty acids suppress mitochondrial translocation to the immunologic synapse and modulate calcium signaling in T cells. *J. Immunol.* 2010. **184**: 5865–5873.

38 **Ho, P. C., Bihuniak, J. D., Macintyre, A. N., Staron, M., Liu, X. J., Amezquita, R., Tsui, Y. C., et al.** Phosphoenolpyruvate is a metabolic checkpoint of anti-tumor T cell responses. *Cell* 2015. **162**: 1217–1228.

39 **McCoin, C. S., Knotts, T. A., Ono-Moore, K. D., Oort, P. J. and Adams, S. H.**, Long-chain acylcarnitines activate cell stress and myokine release in C2C12 myotubes: calcium-dependent and -independent effects. *Am. J. Physiol. Endocrinol. Metab.* 2015. **308**: E990–E1000.

40 **Fan, Y. Y., Fuentes, N. R., Hou, T. Y., Barhoumi, R., Li, X. C., Deutz, N. E. P., Engelen, M. et al.**, Remodelling of primary human CD4+ T cell plasma membrane order by n-3 PUFA. *Br. J. Nutr.* 2018. **119**: 163–175.

41 **Maciolek, J. A., Pasternak, J. A. and Wilson, H. L.**, Metabolism of activated T lymphocytes. *Curr. Opin. Immunol.* 2014. **27**: 60–74.

42 **Angela, M., Endo, Y., Asou, H. K., Yamamoto, T., Tumes, D. J., Tokuyama, H., Yokote, K. et al.**, Fatty acid metabolic reprogramming via mTOR-mediated inductions of PPARgamma directs early activation of T cells. *Nat. Commun.* 2016. **7**: 13683.

43 **van der Windt, G. J., Everts, B., Chang, C. H., Curtis, J. D., Freitas, T. C., Amiel, E., Pearce, E. J. et al.**, Mitochondrial respiratory capacity is a critical regulator of CD8+ T cell memory development. *Immunity* 2012. **36**: 68–78.

44 **Zech, T., Ejsing, C. S., Gaus, K., de Wet, B., Shevchenko, A., Simons, K. and Harder, T.**, Accumulation of raft lipids in T-cell plasma membrane domains engaged in TCR signalling. *EMBO J.* 2009. **28**: 466–476.

45 **Shibata, E., Kanno, T., Tsuchiya, A., Kuribayashi, K., Tabata, C., Nakano, T. and Nishizaki, T.**, Free fatty acids inhibit protein tyrosine phosphatase 1B and activate Akt. *Cell. Physiol. Biochem.* 2013. **32**: 871–879.

46 **Gamberucci, A., Fulceri, R. and Benedetti, A.**, Inhibition of storen-dependent capacitative Ca2+ influx by unsaturated fatty acids. *Cell Calcium* 1997. **21**: 375–385.

47 **Siafaka-Kapadai, A., Hanahan, D. J. and Javors, M. A.**, Oleic acid-induced Ca^{2+} mobilization in human platelets: is oleic acid an intracellular messenger? *J. Lipid Mediat. Cell Signal.* 1997. **15**: 215–232.

48 **Amtmann, E.**, The antiviral, antitumoural xanthate D609 is a competitive inhibitor of phosphatidylcholine-specific phospholipase C. *Drugs Exp. Clin. Res.* 1996. **22**: 287–294.

49 **Edwards-Hicks, J., Apostolova, P., Buescher, J. M., Maib, H., Stanczak, M. A., Corrado, M., Klein Geltink, R. I. et al.**, Phosphoinositide acyl chain saturation drives CD8+ effector T cell signaling and function. *Nat. Immunol.* 2023. **24**: 516–530.

50 **Sun, Y., Dandekar, R. D., Mao, Y. S., Yin, H. L. and Wulfing, C.**, Phosphatidylinositol (4,5) bisphosphate controls T cell activation by regulating T cell rigidity and organization. *PLoS One* 2011. **6**: e27227.

51 **Wijayaratna, D., Ratnayake, K., Ubeysinghe, S., Kankanamge, D., Tennakoon, M. and Karunarathne, A.**, The spatial distribution of GPCR and Gβγ activity across a cell dictates PIP3 dynamics. *Sci. Rep.* 2023. **13**: 2771.

52 **Contrepois, K., Mahmoudi, S., Ubhi, B. K., Papsdorf, K., Hornburg, D., Brunet, A. and Snyder, M.**, Cross-platform comparison of untargeted and targeted lipidomics approaches on aging mouse plasma. *Sci. Rep.* 2018. **8**: 17747.

53 **Cao, Z., Schmitt, T. C., Varma, V., Sloper, D., Beger, R. D. and Sun, J.**, Evaluation of the performance of lipidyzer platform and its application in the lipidomics analysis in mouse heart and liver. *J. Proteome Res.* 2020. **19**: 2742–2749.

54 **Gu, H., Liu, G., Wang, J., Aubry, A. F. and Arnold, M. E.**, Selecting the correct weighting factors for linear and quadratic calibration curves with least-squares regression algorithm in bioanalytical LC-MS/MS assays and impacts of using incorrect weighting factors on curve stability, data quality, and assay performance. *Anal Chem.* 2014. **86**: 8959–8966.

Abbreviations: **CER:** lesser extent ceramide · **CTV:** cell trace violet · **DAG:** diglyceride · **ECAR:** extracellular acidification rate · **FA:** fatty acids · **FCS:** fetal bovine serum · **FFA:** free fatty acids · **IS:** internal standards · **OCR:** oxygen consumption rate · **PBMCs:** peripheral blood mononuclear cells · **PC:** phosphatidylcholine · **PE:** phosphatidylethanolamine · **PFA:** paraformaldehyde · **SF:** synovial fluid · **SM:** sphingomyelin · **TCR:** T-cell receptor · **TG:** triglyceride · **UFA:** unsaturated fatty acids

Full correspondence: J. H. von Hegedus, Department of Rheumatology, Leiden University Medical Center, Albinusdreef 2 Leiden, Utrecht, 2300 RC, Netherlands
e-mail: j.h.vonhegedus@uu.nl